

## SEASONAL SNOWCOVER IN THE FOOTHILLS OF ALASKA'S ARCTIC SLOPE

Glen E. Liston<sup>1</sup>

Snowcover is a dominant feature of Alaska's Arctic Slope for nine months of each year. During 1984-85, a research program was conducted in the headwaters of the Toolik River in the foothills of the Arctic Slope. Observation of meteorological and snowpack characteristics during the winter and spring allowed description of the snowcover's seasonal evolution. This study comprises the most comprehensive and long term snow study to date in Arctic Alaska.

The snowcover of this area was strongly redistributed by southerly winds, in contrast to the predominantly east-west winds occurring in the coastal regions of the Arctic Slope. Snow water equivalent depths ranged from 0 to 150 cm, with a mean depth of 10.3 cm. Snow accumulations on lee slopes of 2 to 3 degrees were 65 percent greater than those on windward slopes of similar angle. This distribution is in contrast to current models predicting profiles of snowdrifts in topographic catchments which predict that the minimum lee slope initiating drift development is about 10 degrees.

In the Arctic, the snowmelt period is the most significant hydrological event of the year. In 1985, melting began on 14 May, and by 31 May, ninety-eight percent of the total snow volume for the site had been melted. The rate of exposure of tundra varies greatly as snowmelt progresses. In this study, a 55 percent decrease in snowcover occurred over a period of only 3 days. This rapid decrease in snowcover is shown to be due to the presence of large areal distributions of uniformly thick snow.

### INTRODUCTION

Seasonal snow is a significant feature of middle and upper latitude environments. On the Arctic Slope of Alaska, seasonal snow is a dominant feature of the landscape for nine months of each year. Several problems have been identified which relate directly to this snowcover. In regions lacking sufficient fresh water supply due to lack of runoff or suitable reservoirs, for instance, there is an interest in accumulating snow into large drifts to serve as summer water sources (Slaughter et al., 1975). In addition, the petroleum industry spends millions of dollars annually, removing snow from materiel sites, drill pads, and roads at their arctic drilling locations. Furthermore, Federal regulations designed to protect underlying arctic vegetation stipulate, based on snowcover amount, when travel across the arctic tundra is permissible. Only through knowledge of arctic snowcover features can this determination be made accurately and thus fulfill its intended objective. Snowcover influences not only the activities of people, but also arctic flora and fauna are affected by its presence. Vegetation growth is influenced by spring and summer snowmelt from drifts formed the previous winter. The depth of snow dictates where caribou can feed, and microtine rodents living beneath the snow depend on it for protection from predators and extremes of wind and temperature in the environment above.

Considering the significant role that winter snowcover plays on the Arctic Slope, little information is available on it in current literature.

---

<sup>1</sup>Grad. Student, Dept. of Civil Engr., Montana State University.

Benson (1967) provided a broad overview of polar regions' snowcover, and addressed the general snowcover of Alaska's Arctic Slope (Benson, 1969). Benson et al. (1975) discussed the snowcover in the Prudhoe Bay area, and Sloan et al. (1979) described the snowcover characteristics of the western half of the Arctic Slope. Wendler (1978) compared the blowing snow and snow precipitation relationships at Barrow and Barter Island, the two National Weather Service stations located on Alaska's northern coast, and found that blowing snow is most frequently associated with wind from the east and west at those stations. Using satellite imagery, air and surface observations, Holmgren et al. (1975) described the characteristics of breakup across the Arctic Slope from the crest of the Brooks Range to the Arctic Ocean. The snow distribution is shown to be largely determined by wind erosion and deposition through drifting, and definite variations in snow accumulation and ablation are found across the Arctic Slope.

This paper describes results relating to the distribution and melting of an arctic winter snowcover found during a year-long research project conducted during 1984-85.

#### SITE DESCRIPTION

This research was conducted in the northern foothills of the Brooks Range, in the area surrounding the head waters of the Toolik River and Imnavait Creek, latitude 68 30' N, longitude 149 15' W (Figure 1). The snow research site covers an area of 17.5 km<sup>2</sup> and was focused on for detailed snow measurements. An isolated watershed covering an area of 2.33 km<sup>2</sup> lies within the snow research area.

The vegetative covering of the research site is composed primarily of low growing sedges and grasses roughly 10 cm in height, with an occasional grouping of taller willows, approximately 25 cm, located in hillside water tracks. Tussock tundra type features prevail over the area. Swampy moss type vegetation commonly grows in the flatter valley bottoms, and dry rocky outcrops exist on the exposed ridges. The site is characterized by gently rolling ridges and valleys with wavelengths of 1 to 2 km and amplitudes of 25 to 75 m. These ridge axes are aligned nearly north-south (350 degrees true). The rolling foothills of the research area lie within the Foothills Region and are similar to roughly one-half of the Arctic Slope (Wahrhaftig, 1965).

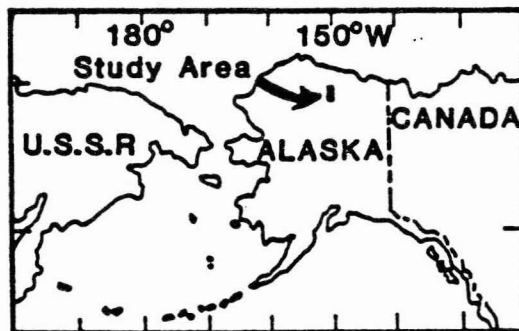


Figure 1. Map of Alaska indicating research site.

#### DESCRIPTION AND ANALYSIS OF THE WINTER SNOWPACK

In wind-swept polar regions, the areal snow distribution pattern represents a measure of the integrated winds and precipitation over a given period of time. To determine the effect of winds on snowcover redistribution, a detailed snow distribution map was produced depicting end-of-winter snow-water-equivalent depths.

#### Topographic Mapping

To aid in the snow distribution mapping, two sets of topographic maps were produced, one covering the research site at a scale of 1:6000 with a 5 m contour interval, and one encompassing part of the isolated watershed, covering an area of 2.4 km<sup>2</sup>, at a scale of 1:1000 with a contour interval of 1 m. In addition to the contour maps, orthophoto maps were made of the site at a scale of 1:6000 and of the watershed area at a scale of 1:1000. These topographic maps have been drawn with sufficient detail that, when superim-

posed onto the orthophoto maps of the same area, it is possible to locate very accurately the positions of measurements and specific features that are of interest in the study.

### Mapping of Snow Distribution

To develop an end-of-winter snow distribution map, snow depths were measured in late March and early May, 1985. Six probe lines were established. These lines ranged in length from 0.2 km to 3.5 km. Snow depths along these lines were measured at 5 m intervals. In addition to these probe lines, snow depth measurements were made at 13 other specific sites, in areas not covered by the probe lines. Details of measurement sites and transects are provided by Liston (1986).

In addition to measurements on the ground, three sets of aerial photographs were taken to observe the 1984-85 winter snowpack. The first set, taken on 6 April, 1985 showed the snowcover at its maximum depth near winter's end. The second set was taken on 21 May, 1985, 6 days into the melt period when 90% of the site was still covered by snow. The third set was taken on 28 May, 1985 when only 20% of the site was covered by snow. Each set of photographs consists of approximately 60 oblique photographs taken at altitudes of 500, 1000, and 3000 m above the tundra surface.

For each of the three sets of aerial photographs, maps were drawn outlining the snow-vegetation boundaries. Locating specific snow-vegetative features, such as drifts and snow and tundra patches, was facilitated by surveyed aerial markers which had been established before the photographs were taken and also by identification of specific terrain features which show up on the orthophoto maps, e.g., ponds, glacial erratics, and rock outcroppings.

The photographs taken on 6 April yield a late winter map identifying three distinct categories of snowcover: areas of 100% exposed rock or vegetation, areas of thin snowcover showing frequent protrusions of vegetation, and areas of continuous snowcover. The photographs taken on 21 and 28 May show the tundra surface when snowmelt had taken place for approximately 6 and 13 days respectively. Both sets of photographs yield maps identifying four snow-vegetative categories across the site: first, areas of continuous snowcover, second, regions with vegetation showing but still greater than 50% snowcover, third, areas with less than 50% snowcover, and finally, areas of 100% exposed vegetation.

The three maps which outline the different snow-vegetative patterns were combined, producing one map outlining snow-vegetative patterns during the three different aerial photographic surveys. On this combined map, all snow depth data from the end-of-winter ground surveys and probe lines were plotted. Analysis of the end-of-winter probe data and the combined snow pattern map showed that this snow pattern map could be used to extrapolate snow depths into regions without probe data. Using the snow pattern map and end-of-winter snow depth data, contour lines of equal snow depth were drawn onto a combination orthophoto-topographic map. This produced an end-of-winter snow distribution map. Contours were drawn at 10 cm intervals for the depth range 0 to 70 cm. For snowpacks deeper than 70 cm, contour intervals of 50 cm were used for depths of 100 to 400 cm. These snow depths were then converted to snow water equivalent as discussed below.

Using an Adirondack Snow Sampling Tube, end-of-winter snowpack water equivalent and snow depth measurements were made at 10 m intervals crossing the isolated watershed (a distance of approximately 0.9 km). The 82 collected values of mean vertical snow density,  $r$ , and depth,  $D$ , are plotted in Figure 2. An average curve fitted to these data can be expressed by the equation,

$$r = 0.00042 * D + 0.234 ; \quad 15 < D < 65 \quad (1)$$

where  $r$  is in  $g/cm^3$  and  $D$  is in cm. The values given by Eq. 1 are roughly 25% less than those given by Benson et al. (1975) for snows on the Arctic Coast near Prudhoe Bay, Alaska, due to the lower wind speeds experienced in this area of the Foothills Region (Liston, 1986).

In addition to the Adirondack method of snow density measurement, snow pits were dug and density profiles were measured throughout the area using

standard CRREL 500 cm<sup>3</sup> snow sampling tubes. In individual snow layers, densities were measured which ranged from 0.18 g/cm<sup>3</sup> to 0.54 g/cm<sup>3</sup>. Consistently, the lowest measured densities were found in a depth hoar layer located within the lowest 20 cm of the snowpack, and in new, loose snow layers at the surface of the snowpack. The highest densities were found to exist in wind slabs and in snowpacks deeper than 70 cm.

To convert mapped snow depths to water equivalence, a density of 0.25 g/cm<sup>3</sup> was used for the snow depth range 0 to 70 cm. At greater depths, in the range 70 to 375 cm, a density of 0.42 g/cm<sup>3</sup> was used. This higher value for density is within 10% of the values given by Benson et al. (1975) based on data collected from drift traps along the Arctic Slope (Benson, 1969; 1982). Contours on a working water equivalent map were drawn at 2.5 cm intervals. Errors are estimated to be  $\pm 1$  contour interval, i.e.,  $\pm 2.5$  cm. Contours on the published water equivalent map (Liston, 1986) were drawn at 5 cm intervals.

Water equivalent contours on the working water equivalent map were digitized using a computer to determine the area enclosed by each contour. A graphical representation of this digitized snow distribution data for the snow research area is found in Figure 3. Water equivalent values range from 0 to 150 cm with 75% of the site covered by the range 7.5 to 12.5 cm. Only 2.3% of the area was covered by more than 20.0 cm of water equivalent. This digitized information was then used to compute mean snow water equivalent values of 10.3 and 10.2 cm, for the snow research area and isolated watershed, respectively.

#### Snow Distribution/Wind Relationships

The end-of-winter snow distribution map allows an analysis of topography and snow distribution relationships. A most striking feature is the large fluctuation in snow depth across the site. Depths range from 0 to 375 cm of snow (0 to 150 cm snow water equivalent). These extremes occur over horizontal distances of only 25 m. From the map, it is obvious that there are definite regions which are favored receptacles for snow deposition and other areas which are favored by erosive processes. One special feature of the erosion and deposition zones shown on the map is that snow accumulations on lee slopes of only 2 to 3 degrees were approximately 65% greater than those of windward slopes of similar angles. This is in contrast to current models predicting profiles of snowdrifts in topographic catchments, developed by Finney (1939), Berg and Caine (1975), and Tabler (1975), which all predict that the minimum embankment slope initiating drift development is about 10 degrees.

The direction of snow transport during erosion and deposition is of

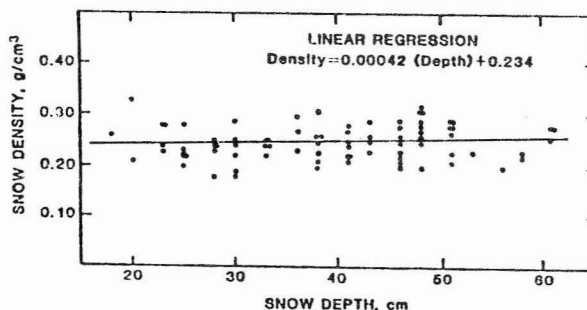


Figure 2. Snow density-depth relationship obtained from an east-west traverse of the isolated watershed.

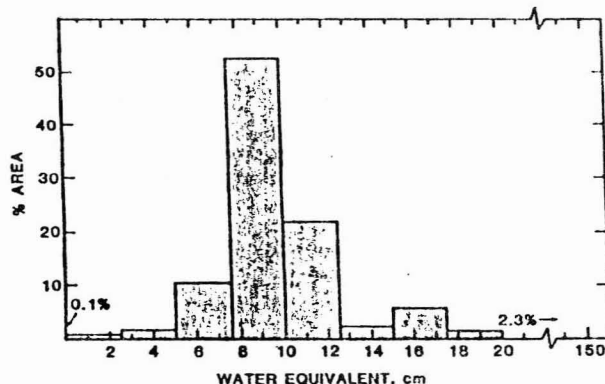


Figure 3. Snow water equivalent distribution as determined from water equivalent map.

primary importance in describing the snow distribution pattern. At this site, obstructions large enough to obstruct air flow and develop measurable drifts are large boulder erratics roughly 2 m in diameter, small portable trailer buildings, and snow piles built up from road clearing work. Measured orientation of drifts built up behind these obstructions suggest two major drift or significant wind events; the larger was caused by winds from 200 degrees, the smaller from 175 degrees. When winds from 175 and 200 degrees are compared with the topographic-snow distribution map, it is clear that these winds have produced the measured snow distribution pattern. Observations of winter satellite imagery show that this southerly flow is due to strong katabatic winds which flow down the north-south trending valleys of the Brooks Range. These winds remove snow from the valley walls and bottoms, and extend for some unknown distance into the foothills of the Arctic Slope (Liston et al., 1986). The strong flow from the south evident in this area is in dramatic contrast to the major snow transporting winds which exist farther north on the Arctic Coastal Plain. In that region, two wind directions, one from the west and one from the east redistribute the majority of snow (Conover, 1960; Benson, 1969; 1982; Wendler, 1978).

#### SNOWMELT PROCESSES

In May, as temperatures of air and snowpack rise, the snow approaches its final modification under the influence of the environment surrounding it. The major snowmelt period on the Arctic Slope lasts 2 to 4 weeks (Benson et al., 1975). The time of snowmelt along the Arctic Coast lags the foothills region by approximately 2 to 3 weeks (Holmgren et al., 1975).

The heat balance components of net radiation, eddy sensible heat flux, heat flux in soil and snow, and the latent heat flux undergo significant changes during the snowmelt period (Weller et al., 1972). One feature of the melt period is the large increase in net radiation which increases the energy available for heating the air and for evaporation. The large difference in albedo between snow and tundra plays a significant role in this increase in net radiation. The absorption of radiation by exposed tundra during the snowmelt period gives rise to small "heat islands" which act as heat sources. Heat emitted by these regions of exposed tundra warms the air above, and local advection carries that heat to the remaining snow. As more tundra is exposed, the amount of absorbed radiation increases, and consequently the heating source feeds back on itself, further accelerating melt.

In 1985, surface melt was initiated on 8 May and continued on 9 May when air temperatures were above freezing for several hours each day. Temperatures below the melting point prevailed during the period 10-13 May. Melting began again on 14 May and continued until the snowcover disappeared. By 31 May, 98% of the total snow volume for the site had been melted. During snowmelt, the rate of exposure of tundra varies greatly with time (Figure 4). A dramatic feature of this graph is the 55% decrease in snowcover over a period of only 3 days.

The melting of snowcover is strongly dependent upon both the local net radiation balance and by the advection of warm and cold air masses, which affect both the long-wave radiation balance and the sensible heat transfer, into the region. To separate the snowmelt contributions of radiation and advection, a detailed micrometeorological and macrometeorological study would be required. In lieu of such a detailed study, the cumulative effect of these processes will be

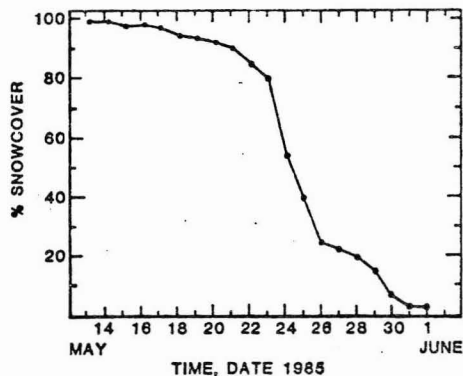


Figure 4. Variation of percentage of snowcover over the melt period.

addressed and discussed.

Melt rate over the snow research area can be determined by the following method. The water equivalent distribution graph (Figure 3) is integrated yielding a plot of percent snowcover as a function of water equivalent (Figure 5). This integrated snow distribution curve can now be directly compared with the percent snowcover as a function of time curve (Figure 4) (note common y-axis) to create a plot of water equivalent as a function of time for the snow research area (Figure 6). The slope of this curve describes the change in snow water equivalent with time, or melt rate.

Figure 6 shows significant short term (daily) and longer term (several days) variation in melt rate, although no general overall acceleration in melt rate is seen as the melt progressed. As a consequence, it is suspected that the melt rate has been affected by factors such as the advection of a cooler air mass into the area, thus masking an acceleration due to the exposing of tundra.

A second procedure for measuring melt rate is to choose a specific site and measure snow water equivalent at that site on a periodic basis. Daily snowpack water equivalents were measured at four specific sites during the melt period (Hinzman, 1986). From these data, daily melt rates were calculated. When these daily melt rates are plotted with average daily temperatures (Figure 7), a significant correlation ( $r^2 = 0.71$ ) is found. Since snowmelt rates are air temperature dependent, air temperature measurements over the melt period can give some indication of the air mass influence on the 1985 melt season.

Figure 7 shows a definite reduction in air temperature starting late in the melt period. In contrast to this, the exposure of bare tundra should only serve to increase air temperatures. The lack of warming, and in fact, the drop in air temperature late in the melt period, indicates that an external cooling mechanism was introduced. This cooling, probably due to advection of a cooler air mass originating over the Arctic Ocean, has served to moderate the warming influence of exposing tundra and produced a relatively uniform melt behavior over the melt period.

In spite of the lack of rapid acceleration of melt late in the period, the area still experienced a rapid decrease in areal snowcover. To help explain this rapid depletion, Figure 6 can be used to determine an average melt rate for the site over the melt period. The plotted points can be described by a straight line of the form

$$H = -1.0 t + 20.9 ; \quad (r^2 = 0.94)$$

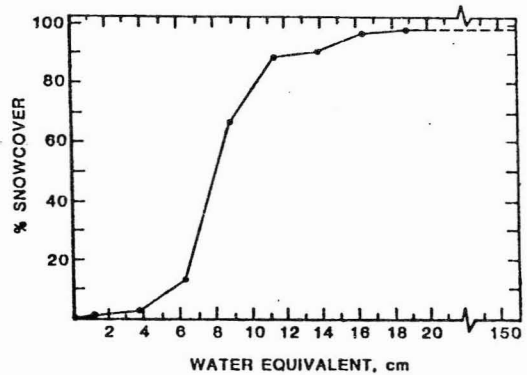


Figure 5. Integrated water equivalent distribution obtained by piecewise integration of water equivalent distribution.

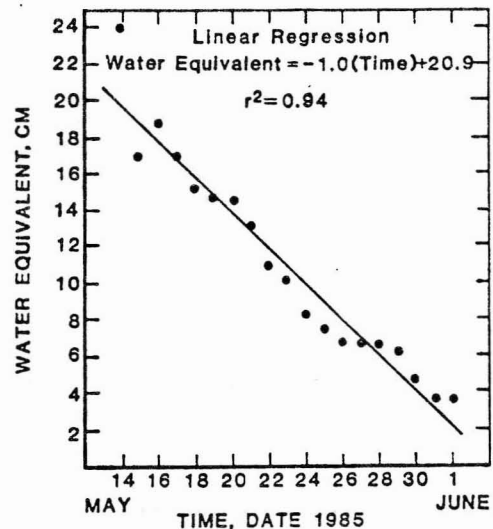


Figure 6. Variation of site water equivalent with time.

where H is snow thickness (cm water equivalent), and t is time (days). The slope of this line gives change in snow thickness due to melting,

$$dH/dt = - 1.0 \quad (3)$$

in cm water equivalent per day. This melt rate can be applied to the water equivalent distribution (Figure 3) and a curve of percent snowcover as a function of time can be generated (Figure 8).

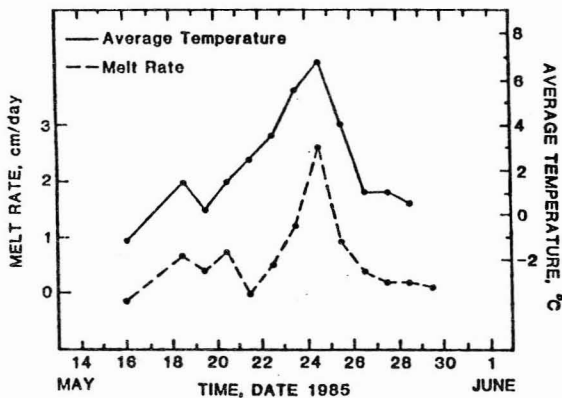


Figure 7. Average daily air temperature and daily melt rate variations over the melt period. (From data collected by Hinzman, 1986).

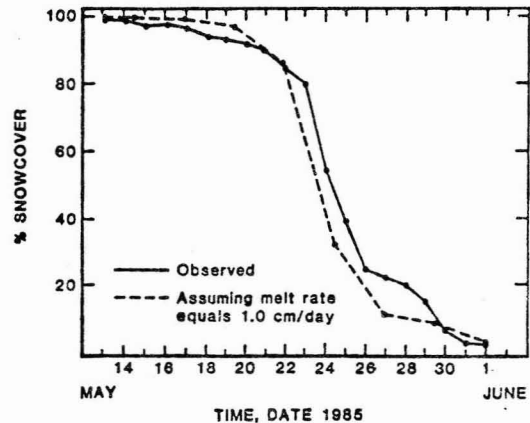


Figure 8. Observed snowcover depletion and snowcover depletion resulting from applying a 1.0 cm/day melt rate to the measured snow distribution.

Figure 8 shows that when a constant melt rate is applied to a snowcover consisting of major portions of uniformly thick snow, a rapid exposure of tundra occurs at critical times. Under the condition of accelerated melt rates resulting from an increase in exposed tundra during the melt period, feedback processes would produce even more rapid exposure of tundra.

The interaction between the large and small scale physical processes which influence snowmelt is complex. A method has been developed, using snowcover depletion and integrated snow water equivalent curves, which allows calculation of the cumulative effect of these processes over a large region over the melt period. Under the condition of unchanging atmospheric circulation pattern, it is expected that as more tundra is exposed, snowmelt will accelerate. Applying the developed method to the 1985 spring melt shows melt rates which are not significantly accelerated as melt progressed. This lack of acceleration appears to be the result of dominating cold air advection into the region late in the period.

#### CONCLUSIONS

During the winter, the snowcover of this area experienced significant redistribution by the wind, resulting in water equivalent depths ranging from 0 to 150 cm. The snow distribution also shows snow accumulations on lee slopes of only 2 to 3 degrees, which were 65% greater than those of windward slopes of similar angle. This significant difference in accumulation on shallow slopes contrasts with current snow drift accumulation models which all predict that the minimum embankment slope initiating drift development is about 10 degrees. Redistribution of snow within the snow research area is the result of katabatic winds flowing north from the Brooks Range. The winds

which redistribute snow on the Arctic Coastal Plain blow from the east and west. Also, it is apparent that average wind speeds experienced in this area of the foothills are much lower than those found near the coast.

Mean end-of-winter water equivalent of the snow for the 1984-85 winter was found to be 10.3 cm. 75% of the site was covered by water equivalent depths in the range 7.5 to 12.5 cm, with 2.3% of the site covered by depths between 20 and 150 cm. The snowcover was characterized by a continuous layer of depth hoar 10 to 15 cm deep, with densities of 0.18 to 0.26 g/cm<sup>3</sup>, overlain by snow which had been modified by wind to varying degrees and having densities of 0.30 to 0.54 g/cm<sup>3</sup>.

Snowmelt rates are shown to be dependent upon air temperature. Therefore, in addition to increased air temperatures resulting from exposure of bare tundra, large scale advection of warm and cold air masses into a region strongly governs snowmelt occurrence and behavior. A method of determining melt over regions of large areal extent was developed. Applying this to the 1985 snowmelt showed that the expected rising of air temperatures resulting from the exposure of bare tundra was counteracted by the advection of a cold air mass into the region late in the melt period.

#### ACKNOWLEDGMENTS

The research reported here was supported by the U. S. Department of Energy's Ecological Research Division. The author would like to express his sincere appreciation for the support and guidance received from Dr. Carl S. Benson and Larry D. Hinzman throughout this research effort.

#### REFERENCES

- Benson, C. S., 1967, "A reconnaissance snow survey of interior Alaska," Geophysical Institute, University of Alaska Report UAG R-190, December 1967, 71 p.
- Benson, C. S., 1969, "The seasonal snow cover of Arctic Alaska," Arctic Institute of North America, Research Paper No. 51, 80 p.
- Benson, C. S., 1982, "Reassessment of winter precipitation on Alaska's Arctic Slope and measurements on the flux of wind blown snow," Geophysical Institute, University of Alaska Report UAG R-288, September 1982, 26 p.
- Benson, C. S., B. Holmgren, R. Timmer, G. Weller and S. Parrish, 1975, "Observations on the seasonal snow cover and radiation climate at Prudhoe Bay, Alaska during 1975," In: Ecological Investigations of the Tundra Biome in the Prudhoe Bay Region, Alaska, J. Brown, ed., Biological Papers of the University of Alaska, Special Report No. 2, pp. 12-50.
- Berg, N., and N. Caine, 1975, "Prediction of natural snowdrift accumulation in alpine areas," Final Report to Rocky Mountain Forest and Range Expt. Station (USFS 19-388-CA), Boulder, Dept. of Geography, University of Colorado, 69 p.
- Conover, J. H., 1960, "Macro- and microclimatology of the Arctic Slope of Alaska," Quartermaster Research and Engineering Center, Environmental Protection Research Division, Tech. Rept. EP-139, 65 p.
- Finney, E. A., 1939, "Snow drift control by highway design," Michigan Engineering Experiment Station, Michigan State College, Bulletin No. 86, pp. 1-58.
- Hinzman, L. D., 1986, Unpublished Data, Water Resource Center, Institute of Northern Engineering, University of Alaska, Fairbanks, Alaska.

Holmgren, B., C. Benson and G. Weller, 1975, "A study of the breakup of the Arctic Slope of Alaska by ground, air and satellite observations," In: Climate of the Arctic, G. Weller and S. A. Bowling, eds., Proc. AAAS-AMS Symp., Fairbanks, Alaska, August 1973, Geophysical Institute, University of Alaska, pp. 358-366.

Liston, G. E., 1986, "Seasonal snowcover of the foothills region of Alaska's arctic slope: a survey of properties and processes," M.S. Thesis, University of Alaska, Fairbanks.

Liston, G. E., G. J. Burger, J. M. Miller and C. S. Benson, 1986, "Snowmelt on Alaska's Arctic Slope as seen by LANDSAT," Cold Regions Hydrology Symp., Fairbanks, Alaska, July 1986, Am. Water Resources Assoc.

Slaughter, C. W., M. Mellor, P. V. Sellmann, J. Brown and L. Brown, 1975, "Accumulating snow to augment the fresh water supply at Barrow, Alaska," Cold Regions Res. and Eng. Lab. Spec. Rept. 217, 21 p.

Sloan, C., D. Trabant and W. Glude, 1979, "Reconnaissance snow survey of the National Petroleum Reserve in Alaska, April 1977 and April-May 1978," U.S. Geol. Survey, Water Resources Investigations Open-File Rept. 79-1342, 31 p.

Tabler, R. D., 1975, "Predicting profiles of snowdrifts in topographic catchments," Proc. 43rd Western Snow Conference, pp. 87-97.

Wahrhaftig, C., 1965, "Physiographic divisions of Alaska," U.S. Geol. Survey Prof. Paper 482.

Weller, G., S. Cubley, S. Parker, D. Trabant and C. Benson, 1972, "The tundra microclimate during snowmelt at Barrow, Alaska," Arctic, V. 24, pp. 291-300.

Wendler, G., 1978, "Snow blowing and snowfall on the North Slope, Alaska," Geophysical Institute, University of Alaska Report UAG R-259, 22 p.